

Effects of addition of cationic ligands in hydrous bismuth oxide on removal of fluoride from aqueous solutions

M. Ranjan^{1,*}, A. L. Srivastav² and Shaktibala³

¹Department of Civil Engineering, Sikkim Manipal University, Sikkim 737 132, India

²Department of Chemistry, Indian Institute of Technology (Banaras Hindu University), Varanasi 221 005, India

³Department of Civil Engineering, Poornima Group of Institutions, Jaipur 302 022, India

Hydrous bismuth oxides (HBO2) have been reported to have anionic sorptive properties. In the present study, removal of fluoride from aqueous solution has been explored for its possible application in drinking water treatment. The performance of fluoride removal from aqueous solutions has been studied by adding four cationic ligands (Fe^{2+} , Mg^{2+} , Ca^{2+} and Cu^{2+}) in the matrix of hydrous bismuth oxide (HBO2). Enhanced fluoride removals properties were observed by addition of cations in hydrous bismuth oxide as compared to hydrous bismuth oxide alone. The pH of the treated water was remained in the range 6.9–9.1, indicating that OH^- ions are not released from the adsorbents during fluoride adsorption. Characterizations of HBO2 and HBO2 with four cationic ligands were achieved by using XRD analyses and the tested powders are found crystalline in nature as they show large and sharp peaks. FTIR analyses of tested materials support the results obtained through XRD analyses. Ca and Mg ions in HBO2 appear to increase the pH of point of zero charge (pHPZC) of the powders.

Keywords: Aqueous solutions, cationic ligands, fluoride removal, hydrous bismuth oxides.

FLUORIDE is one of the most concerned naturally occurring contaminant in groundwater in almost all parts of the world. The impact of fluoride in drinking water may be beneficial or harmful to human, it only depend on the concentration of fluoride. The optimum dosage in drinking water is beneficial to human health, whereas elevated levels from the prescribed limit are harmful to human beings¹. Excessive concentration of fluoride in drinking water has become a major health risk factor for humans. Fluoride contamination in water may be due to natural (geogenic) or anthropogenic factors. Major anthropogenic activities such as the use of phosphate fertilizers, pesticides, sewage and sludge, depletion of groundwater table, etc. are responsible for the increase in concentration of fluoride in groundwater^{2,3}. Recently, few studies^{4,5} have reported that around 25 countries in the world suffer from endemic fluorosis. According to some recent estimates^{6,7}, over 200 million people in the world depend on water for drinking

purpose, which has fluoride concentration more than 1.5 mg/l, which is within the guideline value for fluoride in drinking water⁸. In India, high concentration of fluoride in drinking water was first detected in the groundwater of Nellore, Andhra Pradesh in 1937 (ref. 9). Around 25 million people living in 19 states and all Union Territories of India have been affected and approximately 66 million are at risk, including 6 million children below the age of 14 years¹⁰. The Bureau of Indian Standards (BIS) has recommended 1.0 mg/l as desirable and 1.5 mg/l as permissible limit for fluoride concentration in drinking water. WHO⁶ has prescribed the guideline value for fluoride concentration in drinking water as 1 and 1.2 mg/l for warm and cold climatic regions of the world, respectively. The difference in the fluoride concentration intake between hot and cold climate is because of the difference in the water consumption in the two zones respectively⁵. The human body absorbs fluoride through water, food, drugs, cosmetics, etc. and around 75% contribution of total fluoride comes from drinking water alone¹¹. Calcium of teeth and bones attracts fluoride because of its strong electronegative nature. Therefore, dental and skeletal fluorosis is the major health problem due to high fluoride concentration in drinking water^{1,12}. Different techniques have been reported for the removal of excess fluoride from aqueous solutions. On the basis of their mode of action they can be categorized into three major types, viz. chemical method, adsorption and ion-exchange process. Adsorption has been reported as a simple, economically viable technique for the removal of fluoride from aqueous solutions^{13,14}. Recently, a number of adsorptive materials have been reported the in the literature for the removal of fluoride from aqueous solutions such as modified cellulose fibre¹⁵, polymer/biopolymer composites¹⁶, Fe_2O_3 magnetic nanocomposites¹⁷, bauxite¹⁸, waste iron oxide¹⁹, zeolite²⁰, hydrous bismuth oxide²¹ and hydrous ferric oxide⁵.

Materials and methods

Hydrous bismuth oxides with cationic ligands

Bismuth trioxide (Bi_2O_3 ; molecular weight = 466 g) has been used as the starting material for all the preparations of hydrous bismuth oxide (HBO2) media. Hydrous

*For correspondence. (e-mail: manish040533@gmail.com)

bismuth oxide in the form of yellow precipitate was prepared using the method described similar to that of Fritsche²². First, 0.1 M Bi₂O₃ powder was dissolved in 2 N HCl and then 2 N NaOH solution was mixed in the ratio 1 : 2 to obtain HBO2 media. After a period of 1 h contact time, the supernatant was decanted. Finally, the precipitate was washed several times with distilled water until pH of the supernatant attained neutral condition and chloride content was fully removed. In order to prepare HBO2 with additional cationic ligands, chloride salts of Ca, Mg, Cu and Fe in appropriate quantities to obtain 0.01, 0.02, 0.03, 0.05, 0.07 and 0.10 M solutions were dissolved in 2 N HCl working solution of 0.1 M Bi₂O₃. These amended solutions were similarly mixed with double the volumetric proportion of 2 N NaOH solution to get HBO2 precipitates presumably with the respective cationic ligands. All precipitates were dried at 103 ± 2°C for 24 h to obtain their powdered forms.

Fluoride adsorption experiments

Standard solutions of fluoride were prepared using sodium fluoride salt in distilled water. Sorptive removal of fluoride by HBO2 media has been studied without or with cationic ligands in batch experiments. First, 100 ml of standard fluoride solution (5 mg/l) was mixed in distilled water with the respective sorptive media powders at dose of 50 g/l and allowed a reaction time for 3 h. After this, the samples were filtered through Whatman No. 42 filter paper and the filtrate was analysed for the remaining fluoride concentrations and pH. Triplicate samples were tested and the average value reported. Fluoride concentration in water was determined using ion-meter (Hanna Process Instruments Pvt Ltd, Navi Mumbai, India) with ion selective electrode (ISE) according to the standard method (1998). All experiments were carried out at room temperature (25 ± 2°C). pH of the samples was measured using digital pH meter.

The fluoride removal efficiency of a given powder was calculated as

$$\text{Fluoride removal (\%)} = \left(\frac{C_0 - C_i}{C_0} \right) \times 100, \quad (1)$$

where C_0 and C_i are the initial and equilibrium concentrations of fluoride in solution (mg/l) respectively.

Characterization of adsorptive media

X-ray diffraction (XRD) patterns of the selected media were obtained using an X-ray diffractometer (Philips 1710, The Netherlands). Fourier transform infrared (FTIR) spectra of the prepared materials were obtained using FTIR spectrometer (model: FTIR 8400S (CE), Shimadzu Corporation, Kyoto, Japan). pH of point of

zero charge (pH_{pzc}) of the materials was determined as described previously²³.

Results and discussion

Fluoride removal from water by HBO2 powder without and with cationic ligands

Islam and Patel²⁴ studied fluoride removal by polycinnamamide thorium(IV) phosphate which was synthesized by co-precipitation method and characterized by SEM and FTIR analysis. Sujana and Anand²⁵ evaluated the effectiveness of amorphous iron and aluminum mixed hydroxides in removing fluoride from aqueous solutions. The removal of fluoride was 87.6% under optimum conditions. A series of mixed Fe/Al samples was prepared at room temperature by co-precipitating Fe and Al-mixed salt solutions at pH 7.5. The compositions (Fe : Al molar ratio) of the oxides varied as 1 : 0, 3 : 1, 2 : 1, 1 : 1 and 0 : 1; the samples were characterized by XRD, BET surface area and pH_{pzc}. XRD studies indicated the amorphous nature of the samples and Al(III) incorporation on Fe(III) hydroxides. Batch adsorption studies for fluoride removal on these materials showed that the adsorption capacities of the materials were highly influenced by pH of the solution, temperature and initial fluoride concentration. Sri Vastav *et al.*²¹ found that commercially available Bi₂O₃ powder removes approximately 6% of fluoride only, indicating significant changes in the properties of HBO2 with respect to the original Bi₂O₃ powder.

In the absence of any addition of cations in HBO2 powder, the removal of fluoride ions from water was found to be only around 66%. It is observed that cationic ligand-amended HBO2 powder (0.10 M MgCl₂) gives increased fluoride removal (97%) in comparison to HBO2 powder alone which removes 66.4% of fluoride ions from water. Since F is an anion, therefore it was assumed that the addition of the cations such as Ca, Mg, Cu, Fe can enhance the removal through the attraction forces among opposite charged species in aqueous solution. The pH of treated water using all the powders is in the range 6.6–9.1. Figure 1 shows the performance of fluoride removal by HBO2 (without cationic addition) as well as after addition of cationic ligands (Ca, Mg, Cu and Fe) to HBO2 adsorbent.

The performance of various powders prepared in the presence of different cationic ligands with HBO2, which showed highest percentage of fluoride removal in the range of added cationic concentration (1 : 10 to 1 : 1 on molar basis with respect to Bi) is presented in Table 2.

Characterization

In order to characterize the materials, XRD pattern analyses, FTIR spectroscopic analyses and determination of pH_{pzc} of all powders were performed.

Table 1. Adsorption capacity and other parameters for the removal of fluoride by different sorbents

Adsorbent	pH _{pzc}	Adsorption capacity	Concentration range	Contact time (min)	pH	Temperature (°C)	Reference
Acid-treated spent bleaching earth	–	7.752 mg/g	5–45 mg/dm ³	30	3.5	–	27
Hydroxyapatite	–	4.54 mg/g	2.5 × 10 ⁻⁵ to 6.34 × 10 ⁻² mg/l	–	6.0	–	28
Fluorspar	–	1.79 mg/g					
Activated quartz	–	1.16 mg/g					
Calcite quartz	–	0.39 mg/g					
Basic oxygen furnace slag	–	4.58–8.07 mg/g	1–50 mg/l	35	7.0	25–45	24
Alum sludge	–	5.394 mg/g	5–35 mg/l	240	6.0	32	29
Activated alumina (γ-Al ₂ O ₃)	ca. 8.0	0.86 mmol/g	15–100 mg/l	384–1440	5.0–6.0	30	30
Activated alumina (grade OA-25)	–	1450 mg/kg	2.5–14 mg/l	–	7.0	–	31
Metallurgical-grade alumina	–	12.57 mg/g	–	–	5.0–6.0	20	32
La(III) impregnated on alumina	–	0.350 mM/g	2 mM/l	1200	5.7–8.0	25	33
Alum-impregnated activated alumina	–	40.68 mg/g	1–35 mg/l	90	6.5	25	34
Manganese oxide-coated alumina	7.2 ± 0.1	2.851 mg/g	2.5–30 mg/l	90	7.0 ± 0.2	30 ± 2	35
Hydrous manganese oxide-coated alumina	5.9	7.09 mg/g	10–70 mg/l	120	5.2 ± 0.05	ca. 25	36
Copper oxide-coated alumina (COCA)	–	7.770 mg/g	10 mg/l	1440	–	30 ± 1	37
Magnesia-amended activated alumina	8.6 ± 0.2	10.12 mg/g	5–150 mg/l	180	6.5–7.0	30 ± 1	38
Calcium oxide-modified activated alumina and manganese-oxide modified activated alumina	–	101.01 mg/g and 10.18 mg/g	1–1000 mg/l	2880	5.5	25	39
Alkoxide-origen alumina	–	2.0 mg/g	0–25 mg/l	1440	7.0	30 ± 2	40
Quick lime	–	16.67 mg/g	10–50 mg/l	75	–	25 ± 2	41
Limestone (LS) and aluminium hydroxide impregnated limestone (ALLS)	9.23 and 10.17	43.10 mg/g and 84.03 mg/g	100 mg/l	300	8.0	25	42
Schwertmannite	4.2	50.2–55.3	10–90 mg/l	1440	3.8	30°–22.6	43

pH_{pzc}, pH of point of zero charge.

XRD pattern analyses and estimation of Scherrer crystallite size

Phase identification using XRD relies mainly on the positions of the peaks in a diffraction profile and to some extent on the relative intensities of these peaks. Crystallite size can also cause peak broadening. The well-known Scherrer equation explains peak broadening in terms of incident beam divergence which makes it possible to satisfy the Bragg condition for non-adjacent diffraction planes. Once instrument effects have been excluded, the crystallite size is easily calculated as a function of peak width (specified as the full width at half maximum peak

intensity (FWHM)), peak position and wavelength using the Scherrer equation given below

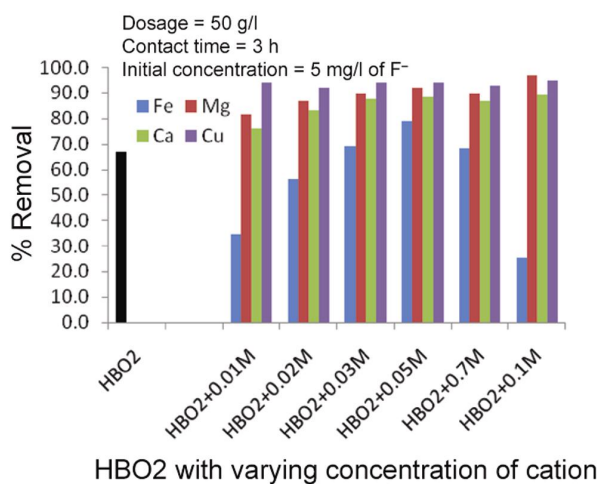
$$D = \frac{0.9 \cdot \lambda}{\text{FWHM} \cdot \cos \theta} \quad (2)$$

where D is the mean particle size (μm), λ the wavelength of X-ray used for diffraction (\AA), FWHM the full width at half maximum peak intensity (2θ) and θ is the angle of diffraction (radians).

As observed from Figure 2a, the XRD pattern of HBO2 shows distinct major peaks at $2\theta = 30.3219$ and 32.8466 radians, indicating crystalline nature

Table 2. Performance of cationic ligands-added HBO2 powders in fluoride removal from water (powder dosage = 50 g/l, contact time = 3 h, initial concentration = 5 mg/l)

Sample combination	Initial composition of aqueous solution			Final composition of aqueous solution			Fluoride removal (%)
	pH	F ⁻ (mg/l)	Cl ⁻ (mg/l)	pH	F ⁻ (mg/l)	Cl ⁻ (mg/l)	
HBO2	8.0	3.99	20.0	7.2	1.34	32	66.4
HBO2 + 0.01FeCl ₃	7.5	5.40	86	7.1	3.52	136	34.70
HBO2 + 0.02FeCl ₃	7.4	5.40	70	6.9	2.36	104	56.22
HBO2 + 0.03FeCl ₃	7.4	5.40	28	6.9	1.65	72	69.40
HBO2 + 0.05FeCl ₃	7.2	5.40	50	6.6	1.15	96	78.70
HBO2 + 0.07FeCl ₃	7.3	5.40	24	6.9	1.70	80	68.50
HBO2 + 0.10FeCl ₃	8.0	5.40	40	7.4	4.02	64	25.40
HBO2 + 0.01MgCl ₂	8.7	3.99	48	8.5	0.73	116	81.70
HBO2 + 0.02MgCl ₂	8.7	3.99	66	8.5	0.53	88	86.71
HBO2 + 0.03MgCl ₂	8.8	3.99	48	8.7	0.41	80	89.72
HBO2 + 0.05MgCl ₂	8.8	3.99	44	8.7	0.31	76	92.23
HBO2 + 0.07MgCl ₂	8.8	3.99	56	8.7	0.41	84	89.72
HBO2 + 0.10MgCl ₂	8.8	3.99	81	8.7	0.12	96	97.00
HBO2 + 0.01CaCl ₂	8.8	2.63	35	8.9	0.63	42	76.00
HBO2 + 0.02CaCl ₂	8.3	2.63	33	8.8	0.44	38	83.30
HBO2 + 0.03CaCl ₂	9.1	2.63	26	9.1	0.32	46	87.80
HBO2 + 0.05CaCl ₂	9.0	2.63	51	9.0	0.30	64	88.60
HBO2 + 0.07CaCl ₂	8.9	2.63	39	9.0	0.35	50	86.70
HBO2 + 0.10CaCl ₂	8.9	2.63	54	9.1	0.28	78	89.4
HBO2 + 0.01CuCl ₂	8.2	3.34	34	7.8	0.20	48	94.00
HBO2 + 0.02CuCl ₂	8.1	3.34	27	7.5	0.24	42	92.00
HBO2 + 0.03CuCl ₂	8.3	3.34	24	7.3	0.20	44	94.00
HBO2 + 0.05CuCl ₂	8.1	3.34	25	7.3	0.20	50	94.00
HBO2 + 0.07CuCl ₂	8.2	3.34	28	7.5	0.26	34	93.00
HBO2 + 0.10CuCl ₂	8.2	3.34	35	7.6	0.14	46	95.0

**Figure 1.** Sorptive percentage removal of fluoride using HBO2 powder without and with Ca, Mg, Cu and Fe cationic ligands.

of HBO2. Using standard JCPDS software²⁶, the chemical composition of HBO2 powder corresponded most closely to Bi(OH)₃ (file no. ID: 01-0898).

XRD of HBO2 powder prepared in presence of 0.10 M CaCl₂ solution: Figure 2 b shows the XRD pattern of HBO2 powder prepared in presence of 0.10 M CaCl₂ solution. The pattern giving several peaks indicates

crystalline character of the HBO2 powder prepared in presence of 0.10 M CaCl₂. The highest peak is observed at $2\theta = 29.5597$ and 30.4950 radians and the chemical composition of the HBO2 powder prepared in presence of 0.10 M CaCl₂ corresponds to Bi₄Ca₅O₂₆ according to file number ID: 42-1460 of JCPDS²⁶. This shows that HBO2 appears to have incorporated calcium ions also in the matrix of the material formed in the presence of 0.10 M CaCl₂ solution.

XRD of HBO2 powder prepared in presence of 0.10 M MgCl₂ solution: Figure 2 c shows the XRD pattern of HBO2 powder prepared in presence of 0.10 M MgCl₂ solution in order to incorporate additional Mg cationic ligands. The highest peak is observed at $2\theta = 32.8563$ and 31.8234 radians and the possible chemical combination of the HBO2 powder prepared in presence of 0.10 M MgCl₂, according to file no. ID: 42-0182 of JCPDS²⁶ is found as Bi₁₂MgO₁₉. Analysis of the compound shows that it is crystalline in character and Mg cationic ligand appears to have been incorporated in HBO2 material matrix.

XRD of HBO2 powder prepared in presence of 0.10 M CuCl₂ solution: Figure 2 d shows the XRD pattern of HBO2 powder prepared in presence of 0.10 M CuCl₂ solution in order to incorporate copper cationic

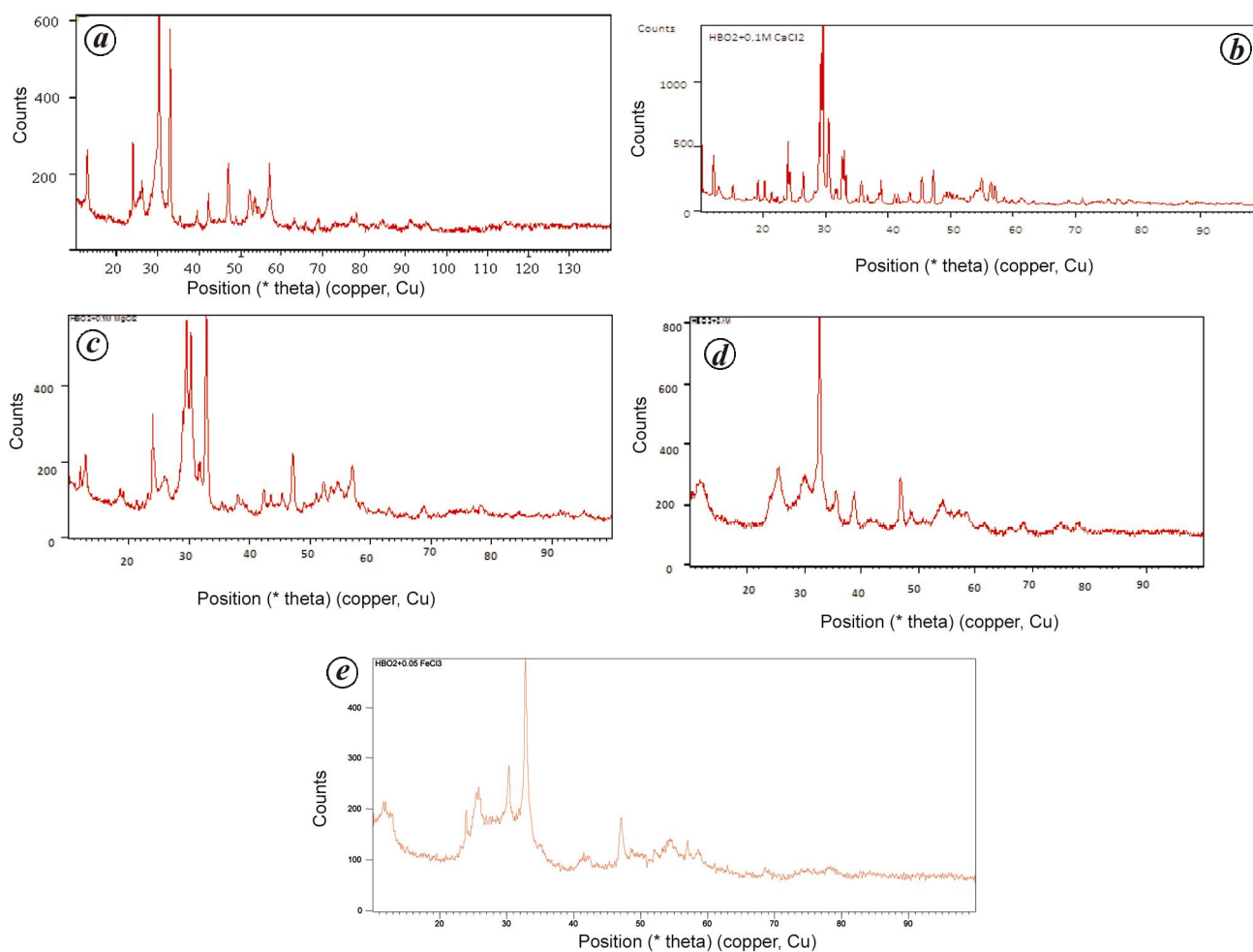


Figure 2. *a*, XRD pattern of HBO2 powder without any cationic ligand ($\text{Bi}(\text{OH})_3$ according to file no. ID: 01-0898)²⁶. *b*, XRD pattern of HBO2 prepared in presence of 0.10 M CaCl_2 solution ($\text{Bi}_4\text{Ca}_5\text{O}_{26}$ according to file no. ID: 42-1460)²⁶. *c*, XRD pattern of HBO2 prepared in presence of 0.10 M MgCl_2 solution ($\text{Bi}_{12}\text{MgO}_{19}$ according to file no. ID: 42-0182)²⁶. *d*, XRD pattern of HBO2 prepared in presence of 0.10 M CuCl_2 solution (CuBi_2O_4 according to file no. ID: 47-0096)²⁶. *e*, XRD pattern of HBO2 prepared in presence of 0.05 M FeCl_3 solution ($\text{Bi}_{24}\text{Fe}_2\text{O}_{39}$ according to file no. ID: 42-0201)²⁶.

Table 3. Results of XRD analyses of HBO2 powder prepared in presence of Ca, Mg, Cu and Fe cationic ligands

Sample powder	Peak enlisted position (2θ)	Possible compound	JCPDS file no.	Scherrer crystallite size (μm)
HBO2	30.3219 32.8466	Bismuth hydroxide	$\text{Bi}(\text{OH})_3$	ID: 01-0898 5.54
HBO2 prepared in presence of 0.10 M CaCl_2 solution	29.5597 30.4950	Calcium bismuth oxide	$\text{Bi}_4\text{Ca}_5\text{O}_{26}$	ID: 42-1460 8.28
HBO2 prepared in presence of 0.10 M MgCl_2 solution	32.8563 31.8234	Megnesium bismuth oxide	$\text{Bi}_{12}\text{MgO}_{19}$	ID: 42-0182 5.54
HBO2 prepared in presence of 0.10 M CuCl_2 solution	32.6760	Copper bismuh oxide	CuBi_2O_4	ID: 47-0096 4.95
HBO2 prepared in presence of 0.05 M FeCl_3 solution	32.7645 46.9908	Bismuth ferric oxide	$\text{Bi}_{24}\text{Fe}_2\text{O}_{39}$	ID: 42-0201 7.53

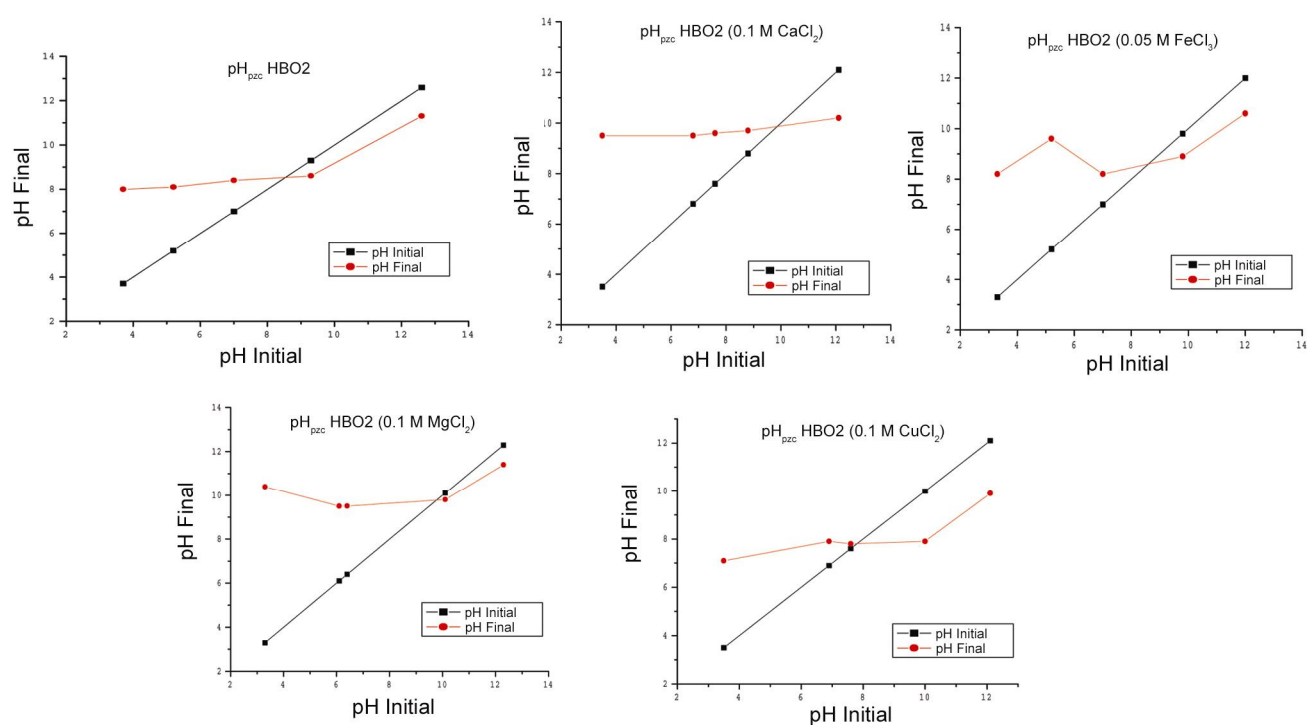


Figure 3. pH_{pzc} of HBO2 powder, and HBO2 powder prepared in the presence of 0.10 M $MgCl_2$, 0.10 M $CaCl_2$, 0.10 M $CuCl_2$ and 0.05 M $FeCl_3$ solution.

Table 4. pH_{pzc} of HBO2 powder prepared under different conditions

Powder sample	pH_{pzc}
HBO2	8.5
HBO2 prepared in presence of 0.10 M $CaCl_2$ solution	9.7
HBO2 prepared in presence of 0.10 M $MgCl_2$ solution	9.7
HBO2 prepared in presence of 0.10 M $CuCl_2$ solution	7.8
HBO2 prepared in presence of 0.05 M $FeCl_3$ solution	8.6

ligands in the matrix. The pattern obtained appears to be significantly different with respect to XRD of HBO2 powder (Figure 2a). The major peak observed at $2\theta = 32.6760$ radians indicates a chemical composition of $CuBi_2O_4$ according to file no. ID: 47-0096 of JCPDS²⁶. The material appears crystalline in character and seems to have incorporated copper ion in the matrix.

XRD of HBO2 powder prepared in presence of 0.05 M $FeCl_3$ solution: Figure 2e shows the XRD pattern of HBO2 powder prepared in presence of 0.05 M $FeCl_3$ solution in order to incorporate additional Fe cationic ligands. The highest peak is observed at $2\theta = 32.7645$ and 46.9908 radians and the possible chemical combination of the material according to file no. ID: 42-0201 of JCPDS²⁶ is found as $Bi_{24}Fe_2O_{39}$. The material formed is crystalline in character and has incorporated Fe ion in the matrix of HBO2 material.

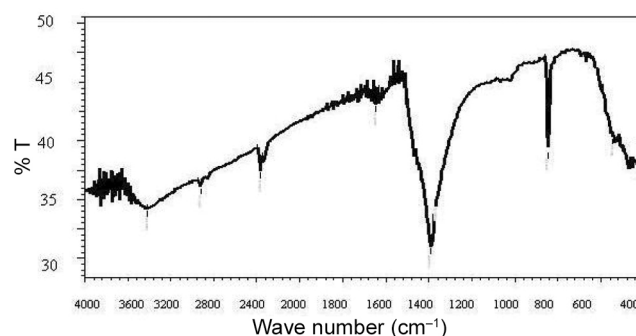


Figure 4. FTIR spectrum of HBO2 powder.

It was also observed that with changing concentration of a cationic ligand in HBO2, the position of highest peak (2θ) changes, but the chemical composition of possible compound indicated by JCPDS²⁶ remains the same. The composition of the suggested compound does not provide any structural detail, but indicates that it is polymeric in nature. The crystallite size calculated using eq. (2) for all the powders is given in Table 3. It is observed that while presence of Cu appears to decrease the mean particle size of HBO2 formed, availability of Ca and Fe cations seems favourable towards increasing the average size of the particle.

pH of point of zero charge (pH_{pzc}): The pH of point of zero charge (pH_{pzc}) is a concept applicable to the adsorption phenomenon describing the concentration of

Table 5. Analyses of enlisted peaks of FTIR spectrum of HBO2

Powder	Peaks enlisted (cm ⁻¹)	Possible metal, functional group present	Range (cm ⁻¹)	Reference	Remarks
HBO2	543.94	Bismuth (Bi)	200–800	44, 45	Bi present
	846.78	–	–	–	
	1361.79				
	1392.65				
	1645.33	Water of hydration	Around 1630	46	
	2359.02	Carbonate	2360–2370	47	
	2920.32	–	–	–	
3419.90	Hydroxyl group (OH)	3400–3800	48	OH group present	

Table 6. Summary of peaks in FTIR spectra of Ca, Mg, Cu and Fe-amended HBO2 powder

Powder	Peaks enlisted (cm ⁻¹)	Possible metal, functional group present	Range (cm ⁻¹)	Reference	Remarks
HBO2 prepared in presence of 0.10 M CaCl ₂ solution	474.50	Bismuth (Bi)	200–800	44, 45	Ca present
	848.76	Calcium oxide (CaO)	412–875	49	
	2359.02	Carbonate	2360–2370	47	
	3655.23, 3851.97	Hydroxyl group (OH)	3400–3800	48	
	1066.67, 1338.64				
	1392.65, 1660.77				
	2274.15, 2330.09				
HBO2 prepared in presence of 0.10 M MgCl ₂ solution	416.64	Bismuth (Bi)	200–800	44, 45	Mg present
	468.72	Magnesium oxide (MgO)	460–510	19	
	1629.90	Water of hydration	Around 1630	20	
	3568.43, 3414.12, 3514.42, 3547.21, 3635.94	Hydroxyl group (OH)	3400–3800	48	
	846.76, 1315.50, 1342.50, 2877.89, 2929.97, 3095.85, 3259.81, 3954.20				
HBO2 prepared in presence of 0.10 M CuCl ₂ solution	430.14	Copper oxide (CuO)	437–606	50	Cu present
	516.94	Bismuth (Bi)	200–800	44, 45	
	1627.97	Water of hydration	Around 1630	20	
	3446.91	Hydroxyl group (OH)	3400–3800	48	
	846.78, 1161.19, 1386.86, 2330.09, 2470.90				
HBO2 prepared in presence of 0.05 M FeCl ₃ solution	549.73	Bismuth (Bi)	200–800	44,45	Fe present
	462.76,	Ferric oxide (FeO)	460–700	48	
	1612.54	Water of hydration	Around 1630	20	
	3394.83, 3425.69,	Hydroxyl group (OH)	3400–3800	48	
	3483.56, 3761.32				
	846.78, 912.36, 1066.67,				
	1357.93, 1390.72,				
	1404.22, 1741.78,				
	2414.96, 2856.67, 3014.84,				
	3043.77, 3207.73, 3232.80,				
3254.02					

hydrogen ion in aqueous solution, such that the electrical charge density on the adsorbent surface is zero. In other words, pH_{pzc} is the pH value at which a solid submerged in an electrolyte exhibits zero net electrical charge on the surface. When the pH of an aqueous environment is lower than pH_{pzc} of the adsorbent, the system is said to be work-

ing ‘below pH_{pzc} ’. Under this condition, the acidic water donates more protons than hydroxide groups, and the adsorbent surface is positively charged (attracting anions). Conversely, above pH_{pzc} , the surface of the adsorbent is negatively charged, attracting cations and repelling anions.

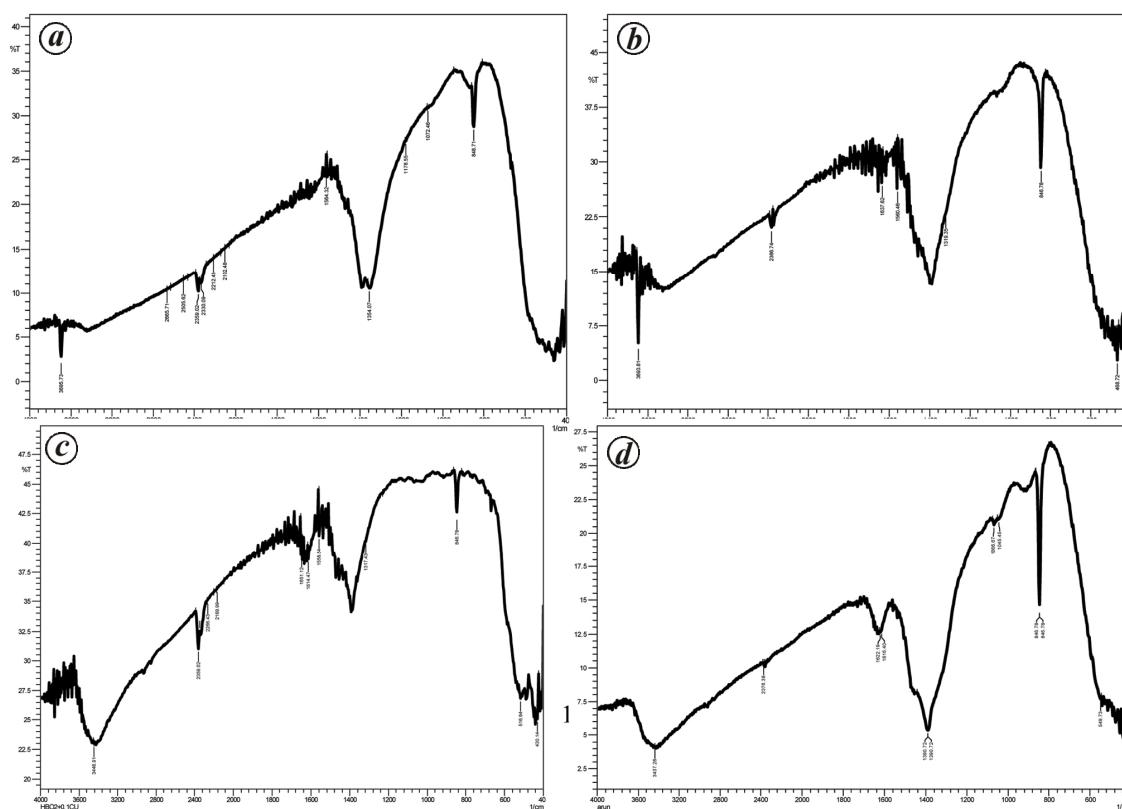


Figure 5. FTIR spectra of HBO2 powder prepared in presence of (a) 0.1 M CaCl₂, (b) 0.1 M MgCl₂, (c) 0.1 M CuCl₂ and (d) 0.05 M FeCl₃ solutions.

To study the surface charge of prepared HBO2 powders, pH_{pzc} was determined following method of Sharma *et al.*²³. For this purpose, 0.01 M NaCl solution was prepared and its initial pH was adjusted between 2.0 and 12.0 using 0.02 N NaOH/HCl solution. Then 50 ml of 0.01 M NaCl was taken in triplicate 250 ml Erlenmeyer flasks and 0.20 g of powder was added in each of them. The contents of the flasks were thoroughly mixed and kept for 48 h. Final pH of the solutions was measured after the contact time using a pH meter. The point of intersection of the line of pH initial with pH final was recorded as pH_{pzc} of the adsorbent material. Figure 3 depicts the curves for HBO2 powder without any added cationic ligand and prepared in presence of 0.10 M MgCl₂ solution. Table 4 presents the pH_{pzc} of all studied HBO2 powders.

As observed from Table 4, while presence of Cu appears to reduce pH_{pzc} of HBO2 powder, Ca, Mg and Fe cations seem to increase the pH_{pzc} values. Higher pH_{pzc} of the material may be beneficial for anionic contaminant removal from aqueous solutions as the surface charge may be positive at all pH values normally found under natural conditions.

Fourier transform infrared spectroscopic analyses: Infrared spectra of HBO2 powders were measured on a Bio-Rad FTS-60 spectrometer in the mid infrared region

(4000–400 cm^{-1}) after 256 scans at 2 cm^{-1} resolution. Samples were prepared by the standard KBr (Merck) pellets method. Figure 4 shows the FTIR spectrum of HBO2 powder. Table 5 presents the summary of enlisted peaks and possible metals and functional groups present in the material. There are peaks indicating the presence of Bi metal, water of hydration and hydroxyl group in HBO2 powder.

Figure 5 a–d depict the FTIR spectra of HBO2 powders prepared in the presence of 0.1 M CaCl₂, 0.1 M MgCl₂, 0.1 M CuCl₂ and 0.05 M FeCl₃ solutions respectively. Table 6 presents the summary of major peaks enlisted in such HBO2 powders prepared in presence of different cationic ligands. The enlisted peaks suggest incorporation of added cationic ligands in HBO2 powder.

Conclusion

Major observations of the experimental results and computational analyses carried out in the present study can be enlisted as follows:

- While HBO2 (prepared by mixing 0.1 M Bi₂O₃ solution in 2 N HCl with twice the volumetric proportion of 2 N NaOH) is yellow in colour and Ca as well as Mg-incorporated HBO2 are also similar, Cu and Fe-amended HBO2 gives dark grey to red colours.

- HBO2 with 0.10 M MgCl₂ solution gives maximum percentage (97) of fluoride removal among the Ca, Mg, Cu and Fe ligands individually at different levels of concentration.
- HBO2 amended with Ca, Mg, Cu or Fe cationic ligand shows improvement in fluoride sorptive potential with respect to unamended form. However, incorporation of Ca and Mg in HBO2 appears to increase pH_{pzc} of the powder, which may be beneficial for application in drinking water treatment. Addition of Cu or Fe tends to decrease pH_{pzc} of HBO2, which may not be favourable for anionic contaminant removal.
- The pH of fluoride-treated water using the same powder remains between 6.9 and 9.1. This indicates that there is no hydroxyl ion exchange from HBO2 powders due to fluoride ion sorption.
- The Cu-incorporated HBO2 tends to decrease the pH of treated water with respect to pH of treated water with HBO2 incorporated with Ca or Mg.
- XRD analyses of HBO2 powder, along with its Ca²⁺, Mg²⁺, Cu²⁺ and Fe²⁺ cations incorporated forms suggest crystalline character of materials. Analysis of chemical composition using appropriate methods²⁶ indicates presence of these cations in HBO2 mixture. HBO2 appears to become more polymerized in presence of such cations. The Scherrer crystallite size of the prepared powders varies in the range 5.54–8.28 μm and the size appears to marginally improve in presence of Mg and Fe.
- It is observed that most of the compounds are polymeric forms of bismuth and cations ligands have attached themselves in the HBO2 polymeric structure.
- FTIR spectra analyses of HBO2 without and with cations indicate distinctive absorption bands corresponding to oxides of added ligands in addition to those of bismuth and hydroxyl ions. Thus, added cationic ligands appears to have become an integral part of the HBO2 compound.

An indicative experiment in which the used HBO2 powder was amended with presence of all the four studied cations (0.01 M Ca, 0.10 M Mg, 0.10 M Cu and 0.05 M Fe) showed around 30% increase in fluoride sorptive potential with respect to unamended HBO2 powder. Thus, the addition of these individual cationic ligands is found to be beneficial.

1. Venkata Mohan, S., Ramanaiah, S. V., Rajkumar, B. and Sarma, P. N., Removal of fluoride from aqueous phase by biosorption onto algal biosorbent *Spirogyra* sp.-IO2: sorption mechanism elucidation. *J. Haz. Mater.*, 2007, **141**, 465–474.
2. EPA, Public health global for fluoride in drinking water, United States Environment Protection Agency, Washington DC, 1997.
3. Ramanaiah, S. V., Venkata Mohan, S., Rajkumar, B. and Sarma, P. N., Monitoring of fluoride concentration in groundwater of Prakasham District in India: correlation with physico-chemical parameters. *J. Environ. Sci. Eng.*, 2006, **48**, 129–134.
4. Chakraborti, Das, B. and Matthew, M. T., Examining India's groundwater quality management. *Environ. Sci. Technol.*, 2011, **45**, 27–33.
5. Sujana, M. G., Mishra, A. and Acharya, B. C., Hydrous ferric oxide doped alginate beads for fluoride removal: adsorption kinetics and equilibrium studies. *Appl. Surf. Sci.*, 2013, **270**, 767–776.
6. WHO, Guidelines for drinking-water quality. First addendum to third edition, 2005; http://www.who.int/water_sanitation_health/dwg/gdwq0506.pdf
7. Ahn, J. S., Geochemical occurrences of arsenic and fluoride in bedrock groundwater: a case study in Geumsan County, Korea. *Environ. Geochem. Health*, 2012, **34**, 43–54.
8. WHO, WHO Guidelines for Drinking Water Quality, Health Criteria and other Supporting Information, World Health Organization, Geneva, 1996, vol. 2, 2nd edn, pp. 231–237.
9. Short, H. E., McRobert, G. R., Bernard, T. W. and Mannadiyar, A. S., Endemic fluorosis in the Madras Presidency. *Ind. J. Med. Res.*, 1937, **25**, 553–561.
10. Sangam, Combating fluorosis with household filters. Newsletters of UN Inter Agency-Working Group on Water and Environmental Sanitation in India, UNICEF, 2003, pp. 1–2.
11. Sarala, K. and Rao, P. R., Endemic fluorosis in the Village Ralla, Anantapuram in Andhra Pradesh – an epidemiological study. *Fluoride*, 1993, **26**, 177–180.
12. Susheela, A. K., Kumar, A., Betnagar, M. and Bahadur, M., Prevalence of endemic fluorosis with gastrointestinal manifestations in people living in some North-Indian villages. *Fluoride*, 1993, **26**, 97–104.
13. Kang, J., Li, B., Song, J., Li, D., Yang, J., Zhan, W. and Liu, D., Defluoridation of water using calcined magnesia/pullulan composite. *Chem. Eng. J.*, 2011, **166**, 765–771.
14. Swaina, S. K., Tanushree Patnaik, P. C., Patnaik, Usha Jha and Dey, R. K., Development of new alginate entrapped Fe(III)–Zr(IV) binary mixed oxide for removal of fluoride from water bodies. *Chem. Eng. J.*, 2013, **215–216**, 763–771.
15. Tian, Y. *et al.*, Modified native cellulose fibers – a novel efficient adsorbent for both fluoride and arsenic. *J. Hazard. Mater.*, 2011, **185**, 93–100.
16. Karthikeyan, M., Satheesh Kumar, K. K. and Elango, K. P., Batch sorption studies on the removal of fluoride ions from water using eco-friendly conducting polymer/bio-polymer composites. *Desalination*, 2011, **267**, 49–56.
17. Bhaumik, M., Leswif, T. Y., Maity, A., Srinivasu, V. V. and Onyango, M. S., Removal of fluoride from aqueous solution by polypyrrole/Fe₃O₄ magnetic nanocomposite. *J. Hazard. Mater.*, 2011, **186**, 150–159.
18. Sujana, M. G. and Anand, S., Fluoride removal studies from contaminated groundwater by using bauxite. *Desalination*, 2011, **267**, 222–227.
19. Huang, Y.-H., Shih, Y.-J. and Chang, C.-C., Adsorption of fluoride by waste iron oxide: the effects of solution pH, major coexisting anions, and adsorbent calcinations temperature. *J. Hazard. Mater.*, 2011, **186**, 1355–1359.
20. Zhang Z., Tan, Y. and Zhong, M., Defluorination of wastewater by calcium chloride modified natural zeolite. *Desalination*, 2011, **276**, 246–252.
21. Srivastav, A. K., Singh, P. K., Srivastav, V. and Sharma, Y. C., Application of a new adsorbent for fluoride removal from aqueous solutions. *J. Hazard. Mater.*, 2013; <http://dx.doi.org/10.1016/j.jhazmat.2013.04.017>.
22. Fritsche, U., Removal of nitrates and other anions from water by yellow bismuth hydroxide. *J. Environ. Sci., Health*, 1993, **A28**(9), 1903–1913.
23. Sharma, Y. C., Uma and Upadhyay, S. N., Removal of a cationic dye from wastewaters by adsorption on activated carbon developed from coconut coir. *Energy Fuels*, 2009, **23**, 2983–2988.

24. Islam, M. and Patel, R., Thermal activation of basic oxygen furnace slag and evaluation of its fluoride removal efficiency. *Chem. Eng. J.*, 2011, **169**, 68–77; doi:10.1016/j.cej.02.054.
25. Sujana, M. G. and Anand, S., Iron and aluminium based mixed hydroxides: a novel sorbent for fluoride removal from aqueous solutions. *Appl. Surf. Sci.*, 2010, **256**, 6956–6962.
26. JCPDS, Now International Centre for Diffraction Data, 12 Campus Boulevard, Newtown Square, PA 19073-3273, USA.
27. Mahramanlioglu, M., Kizilcikli, I. and Bicer, I. O., Adsorption of fluoride from aqueous solution by acid treated spent bleaching earth. *J. Fluorine Chem.*, 2002, **115**, 41–47.
28. Fan, X., Parker, D. J. and Smith, M. D., Adsorption kinetics of fluoride on low cost materials. *Water Res.*, 2003, **37**, 4929–4937.
29. Sujana, M. G., Thakur, R. S. and Rao, S. B., Removal of fluoride from aqueous solution by using alum sludge. *J. Colloid Interface Sci.*, 1998, **206**, 94–101.
30. Ku, Y. and Chiou, H.-M., The adsorption of fluoride ion from aqueous solution by activated alumina. *Water Air Soil Pollut.*, 2002, **133**, 349–361.
31. Ghorai, S. and Pant, K. K., Investigations on the column performance of fluoride adsorption by activated alumina in a fixed-bed. *Chem. Eng. J.*, 2004, **98**, 165–173.
32. Pietrelli, L., Fluoride wastewater treatment by adsorption onto metallurgical grade alumina. *Anal. Chim.*, 2005, **95**, 303–312.
33. Puri, B. K. and Balani, S., Trace determination of fluoride using lanthanum hydroxide supported on alumina. *J. Environ. Sci. Health, Part A*, 2000, **35**, 109–121.
34. Tripathy, S. S., Bersillon, J.-L. and Gopal, K., Removal of fluoride from drinking water by adsorption onto alum-impregnated activated alumina. *Sep. Purif. Technol.*, 2006, **50**, 310–317.
35. Maliyekkal, S. M., Sharma, A. K. and Philip, L., Manganese-oxide-coated alumina: a promising sorbent for defluoridation of water. *Water Res.*, 2006, **40**, 3497–3506.
36. Teng, S.-X., Wang, S.-G., Gong, W.-X., Liu, X.-W. and Gao, B.-Y., Removal of fluoride by hydrous manganese oxide-coated alumina: performance and mechanism. *J. Hazard. Mater.*, 2009, **168**, 1004–1011.
37. Bansiwala, P. P., Biniwale, R. B. and Rayalu, S. S., Copper oxide incorporated mesoporous alumina for defluoridation of drinking water. *Micropor. Mesopor. Mater.*, 2010, **129**, 54–61.
38. Maliyekkal, S. M., Anshup, K. R. and Pradeep, T. A., High yield combustion synthesis of nanopowders. *Malaysian J. Anal. Sci.*, 2010, **11**, 294–301.
39. Camacho, L. M., Torres, A., Saha, D. and Deng, S., Adsorption equilibrium and kinetics of fluoride on sol-gel-derived activated alumina adsorbents. *J. Colloid Interface Sci.*, 2010, **349**, 307–313.
40. Kamble, S. P., Deshpande, G., Barve, P. P., Rayalu, S., Labhsetwar, N. K., Malyshev, A. and Kulkarni, B. D., Adsorption of fluoride from aqueous solution by alumina of alkoxide nature: batch and continuous operation. *Desalination*, 2010, **264**, 15–23.
41. Islam, M. and Patel, R. K., Evaluation of removal efficiency of fluoride from aqueous solution using quick lime. *J. Hazard. Mater.*, 2007, **143**, 303–310.
42. Jain, S. and Jayaram, R. V., Removal of fluoride from contaminated drinking water using unmodified and aluminium hydroxide impregnated blue limestone waste. *Sep. Sci. Technol.*, 2009, **44**, 1436–1451.
43. Eskandarpour, O. M. S., Ochieng, A. and Asai, S., Removal of fluoride ions from aqueous solution at low pH using Schwertmannite. *J. Hazard. Mater.*, 2008, **152**, 571–579.
44. Fruth, V., Popa, M., Berger, D., Ionica, C. M. and Jitianu, M., Phases investigation in the antimony doped Bi₂O₃ system. *J. Eur. Ceram. Soc.*, 2004, **24**, 1295–1299.
45. Ramli, I., Tze, C. M. and Hin, T. Y., Effect of sodium hydroxide concentration on the physico-chemical characteristic of α -Bi₂O₃ nanocrystals. *Solid State Sci. Technol.*, 2007, **15**(1), 30–42.
46. Zhang, W. L., Tian, Z. X., Zhang, N. and Li, X. Q., Nitrate pollution of groundwater in northern China. *Agric. Ecosyst. Environ.*, 1996, **59**, 223–231.
47. Biswas, K., Gupta, K., Goswami, A. and Ghosh, U. C., Fluoride removal efficiency from aqueous solution by synthetic iron (III)–aluminum (III)–chromium (III) ternary mixed oxide. *Desalination*, 2010, **255**, 44–51.
48. Caki, Milorad, D., Nikoli, Goran, S. and Ili, L. A., FTIR spectra of iron(III) complexes with dextran, pullulan and inulin oligomers. *Bull. Chem. Technol. Macedonia*, 2002, **21**(2), 135–146.
49. Bosch Reig, F., Gimeno Adelantado, J. V. and Moya Moreno, M. C. M., FTIR quantitative analysis of calcium carbonate (calcite) and silica (quartz) mixtures using the constant ratio method. Application to geological samples. *Talanta*, 2002, **58**, 811–821.
50. Muhamad, E. N., Irmawati, R., Abdullah, A. H., Taufiq-Yap, Y. H. and Abdul Hamid, S. B., Effect of number of washing on the characteristics of copper oxide nanomagnesia and its application for fluoride removal. *Sci. Total Environ.*, 2010, **408**, 2273–2282.

Received 14 November 2014; revised accepted 7 January 2015